p-ISSN: 1907-8056
e-ISSN: 2527-5410
AGROINTEK
Jurnal Teknologi Industri Pertanian
journal homepage: journal.trunojoyo.ac.id/agrointek

Utilization of sorghum bagasse modified with citric acid for fe(III) adsorption: kinetics and isotherm studies

Bernadeta Ayu Widyaningrum[1*], Tamara Matilda[2], Riska Surya Ningrum[1], Dwi Ajias Pramasari[1]

[1]*Research Center for Biomass and Bioproduct, National Research and Innovation Agency (NRIA), Bogor, Indonesia*
[2]*Bioprocess Engineering, Universitas Brawijaya, Malang, Indonesia*

Article history
Received:
7 April 2022
Revised:
29 May 2022
Accepted:
3 June 2022

Keyword
Adsorption;
modified bagasse sorghum;
Fe(III)ions;
kinetics;
isotherm;

ABSTRACT

In this study, the biomass waste of bagasse sorghum was utilized as adsorbent to reduce heavy metal. Bagasse sorghum was modified using citric acid to enhance the adsorption of Fe(III) ions. The surface morphology, surface functionality, the surface area, and the pore size distribution were identified by using field emission scanning electron microscope (FESEM), Fourier transforms infrared spectroscopy (FTIR) and Brunauer and Teller (BET), and BJH method, respectively. The adsorption parameters were examined. Kinetics and isotherm were also evaluated. The kinetics models fitted well to the pseudo-second-order model, indicating the adsorption mechanism of Fe(III) onto the modified bagasse sorghum (MBS) was chemisorption supported by the Elovich model. The isotherm study was described well by the Freundlich model (R2 = 0.941) with maximum adsorption of 45.872 mg.g-1. It was shown that the low-cost natural adsorbent MBS has potential as a new promising biodegradable adsorbent for Fe(III) removal from aqueous solution

* Corresponding author
Email : detta9.ay@gmail.com
DOI 10.21107/agrointek.v16i4.14273

INTRODUCTION

Untreated industrial waste is the main contributor to heavy metal contaminants in waters. The contamination of heavy metals could cause several problems to the environment and ecosystem health (Khosravihaftkhany et al., 2015). The ferrous (Fe(III)) ions are one of the heavy metals that are dangerous and need to be handled seriously. The Fe(III) ions can be found in ore mining activities, corrosion of water pipes, steel industry, pesticides, ceramics, and batteries (Nurhayatun Nafsiyah, Anis Shofiyani, 2017). The WHO gives the maximum standard of Fe(III) in the drinking water, about 0.3 mg/L. The excessive Fe(III) ions in human bodies can cause anorexia, diabetes mellitus, liver cancer, and other serious diseases (Anbia and Amirmahmoodi, 2016). Standard techniques to remove heavy metal contaminants include ion exchange, adsorption, reverse osmosis, solvent extraction, and chemical precipitation (Ghosh et al., 2011, Shaidan et al., 2012, Lo et al., 2012, Wang et al., 2014). Adsorption is a promising method that is cost-effective, simple, easy to use and requires no additional pollution (Liu et al., 2015). One of the adsorption processes that can remove heavy metals can occur through the interaction between biomass and metal waste; this process can be called biosorption. The dead or waste biomass, live plants, and bacteria are candidates for biosorbent with different adsorption capabilities (Das et al., 2008). Sawdust, wheat husk, maize corn cob, sugarcane bagasse, orange peels, groundnut shells, coconut shells, waste gayo coffee, spent green tea leaves, and walnut shells have been reported as potential biosorbent (Das et al., 2008, Almasi et al., 2012, De Gisi et al., 2016, Segovia-Sandoval et al., 2018, Mariana et al., 2019, 2021, Tejada-Tovar et al., 2021, Jóźwiak et al., 2021). The utilization of biomass as an adsorbent due to its abundance and low cost.

Sorghum bagasse (SB) is an agricultural waste from the sugar industry that consists of three biological polymers (cellulose, hemicellulose, and lignin) (Sun, 2010). SB contains 58.23% cellulose, 25.42% hemicellulose, and 14.95% lignin. Lignocellulosic has functional groups: carboxyl groups, and hydroxyl groups, to bind with metal ions (Sun, 2010). Pre-treatment of biomass has been modified to increase the porosity and surface area due to the removal of lignin, hemicellulose, and cellulose crystallinity in the adsorbent (Xu et al., 2013). Various chemical treatments have been used to modify biomass, such as sulfuric acid, hydrochloric acid, nitric acid, citric acid, tartaric acid, and phosphoric acid (Wan Ngah and Hanafiah, 2008). The enlarged pore size of the biomass during the modification process could also be induced the metal ions will easily enter the pores of the biomass (Suhendrayatna and Zaki, n.d., Wartelle and Marshall, 2000). Citric acid is one of the chemicals rich in hydroxyl and carboxyl groups that have the advantage of modifying the biomass. The functional group of citric acid on the biomass surface could interact with metal ions during removing heavy metal pollutants (Monroy-Figueroa et al., 2014). In previous studies, Sandoval *et al.* (2018) used citric acid to treat the walnut shells for removal of Zn(II), and the adsorption capacity of treated walnut shells was enhanced 2.5 fold (Segovia-Sandoval et al., 2018). Hoang *et al.* (2021) demonstrated their adsorbent: sugarcane bagasse treated with citric acid for Pb(II) adsorption with an adsorption capacity of around 97 mg/g (Hoang et al., 2021). The above results reveal that chemically modified using citric acid could use as a treated adsorbent. In this study, sorghum bagasse (SB) as a potential sorbent was modified with citric acid and applied to reduce the Fe(III) adsorption in the aqueous solution. Several parameters: pH, contact time, adsorbent concentration, and the initial metal concentration, were evaluated. Adsorption kinetics and isotherm models were analyzed for the adsorption performance of modified SB. These results may affect the reduced Fe(III) in the aqueous solution.

METHOD

Materials

Sorghum bagasse, citric acid (Merck), sodium acetate (CH_3COONa) (Merck), and Iron (III) chloride hexahydrate ($FeCl_3.5H_2O$) (Merck). All other chemicals and reagents used in the experiments were analytical grade. Distilled water was used throughout the experiment.

Preparation of modified sorghum bagasse and characterization

Sorghum bagasse (SB) was collected from the Research center for biotechnology and was washed several times to remove the impurities. It was dried at 60^{o}C for 24h. after that. It was ground and sieved to obtain a particle with a size of 0.841mm. The SB was treated chemically using citric acid (CA). 75 gr of SB was immersed in 1000mL of CA (3 M) under a stirrer for 4h at a

temperature of 60°C. Then, the mixer was cooled to room temperature following filtration. The solid SB was heated at a temperature of 80°C for 24h. after that, the temperature was increased to 110°C for 3h. The modified SB (MBS) was washed until it reached neutral pH to remove the excess CA. Then, the MBS was dried at 60°C for 24 h, sealed, and stored for later use in characterization and adsorption studies.

The morphology of sorghum bagasse (SB) and modified sorghum bagasse (MSB) were examined using Field emission scanning electron spectroscopy (FESEM, Thermo Scientific Quattro S). The Brunauer and Teller (BET) and BJH methods determined the surface area and the pore size distribution. The surface functional group was analyzed using Fourier transform infrared spectroscopy (FTIR, Perkin Elmer) with an attenuated total reflectance method at a resolution of 4 cm-1 in the 400 cm-1 – 4000 cm-1.

Determination of pH at point of zero charges (pH_{PZC})

The pH of the point of zero charges (pH_{PZC}) was determined using a pH meter (metrohm) based on the previous method (Oliveira et al., 2021). Specifically, 0.01 M NaCl was adjusted to pH between 2 and 10 using 0.1 M HCl or NaOH. 150 mg samples were mixed with 50 mL of each solution followed by agitation at 150 rpm for 48 h. The pH of the supernatant was then measured, and pH_{PZC} is the point where a plot of pH final vs. pH initial crosses the line pH last = pH initial.

Study adsorption

The adsorption experiment was obtained in a batch adsorber using an Erlenmeyer flask of 350 mL with a volume of 100 mL and a stirring speed of 150 rpm. The effect of parameters such as pH, adsorbent dosage, contact time, and initial concentration was analyzed. The effect of pH was studied in a range of 2 – 6, and the amount of adsorbent dosage was 0.6 – 6 g.L-1. For the effect of contact time, the mixture of SB and Fe(III) was shaking at a different time from 1 to 240 min; then the data fitted to kinetic, the effect of initial concentration of Fe(III) was 60 – 420 mg/L, the data then used to assess isotherm study. The removal of Fe(III) and the adsorption capacity of MBS on Fe(III) were calculated using equations 1 and 2,

$$Fe\ (III)\ removal\ (\%) = \frac{C_e - C_0}{C_0} \quad (1)$$

$$q_e(mg/g) = \frac{(C_e - C_0) \times V}{m} \quad (2)$$

where Co and Ce are the initial and final concentrations (mg/L) of Fe(III), V is the volume of Pb(II) (L), and m is a dose of the adsorbent (g).

Adsorption kinetics

Kinetics are needed to determine the time it takes the system to achieve equilibrium. The adsorption kinetic was analyzed using the pseudo-first-order model (PFO), pseudo-second-order model (PSO), Elovich, and intraparticle diffusion. The equations of kinetic models are in Table 1.

Adsorption isotherms

The adsorption isotherms describe the adsorbate-adsorbent interaction. In these studies, the mathematical models of Langmuir, Freundlich, Temkin, and Dubinin–Radushkevich (D–R) were used to fit the experimental data obtained. The equations of kinetic models are in Table 2.

RESULT AND DISCUSSION

Morphology and BET analysis

SEM was performed to observe the morphology of BS and MBS before and after treatment using CA. The SEM micrograms of BS and MBS are presented in Figure 1, which both show compact and rough surfaces with layering fibers. The changes in morphology can be observed, whereby the surface of MBS was porous and smoother than BS. This indicates that chemical treatments using CA has been successfully modified the morphology due to the removal of wax and other extractives from the surface and also help fill up the pores (Zhong et al., 2012). These pores may have favored for removal of Fe(III) as active sites and increased their surface area. The surface area confirmed the dense structure of SB to be 0.428 m^2/g with total pores of 0.0022 cm^3/g, and for MBS, the surface area of 0.290 m^2/g with entire pores of 0.0015 cm^3/g. This result is similar to previous studies where natural bagasse has a fibrous and compact structure; after chemical treatment, some parts of the fibrous degrade, and there are many pore holes (Tahoon et al., 2020, Leon et al., 2020).

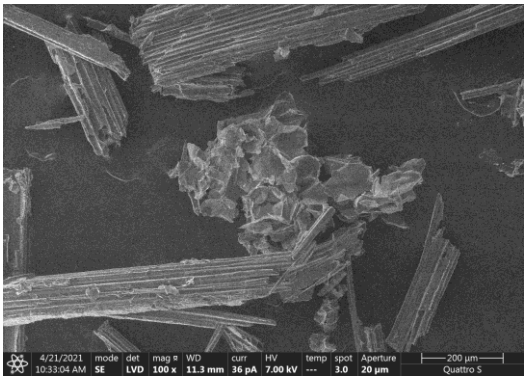

A

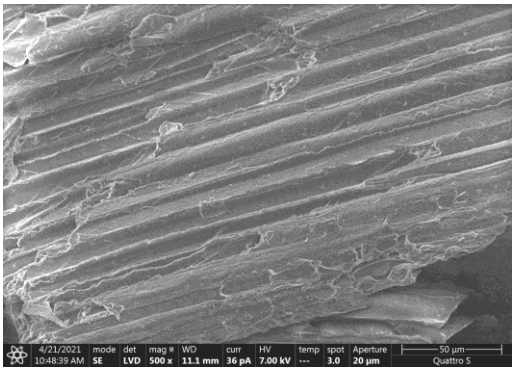

B

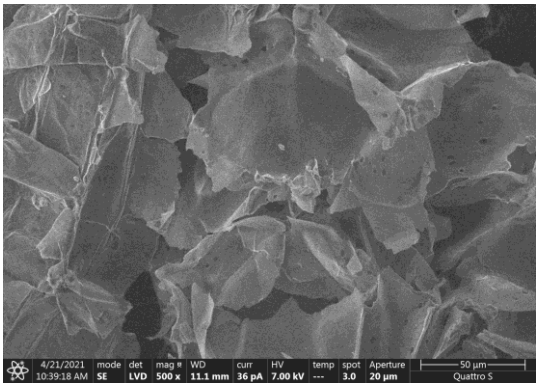

C

Figure 1 The SEM image of (A) SB, (B), and (C) MBS

FTIR analysis

The functional group of SB and MSB was performed by FTIR analysis. The spectra of SB and MSB showed in Figure 2. The spectra exhibit a characteristic peak of lignocellulosic (cellulose, hemicellulose, and lignin). The presence of adsorption around 3300 cm^{-1} is attributed to stretching vibration of OH group, a hydrogen bond or H_2O; band around 2921 to 2850 cm^{-1} corresponds to -CH of an aliphatic group; band around 1720 cm^{-1} is attributed to C=O bond of the carboxyl groups; band around 1628 cm^{-1} is associated to CH_2 symmetric bending; 1367 and 1362 cm^{-1} associated to C-H bending and O-H bending; and a sharp peak at 1019 cm^{-1} corresponding to C-O vibration (Dungani et al., 2016, De Gisi et al., 2016, Candido and Gonçalves, 2016). As presented in Figure 2, the changes in the intensity of the peak at 1720 cm^{-1} suggest that esterification occurred between carboxylic groups of citric acid and hydroxyl groups in cellulose, hemicellulose, and lignin in MBS (Nurfahmi et al., 2016). These suggest that the carboxylic group, C-O-H bending, and C-O vibration could support the adsorbed Fe(III).

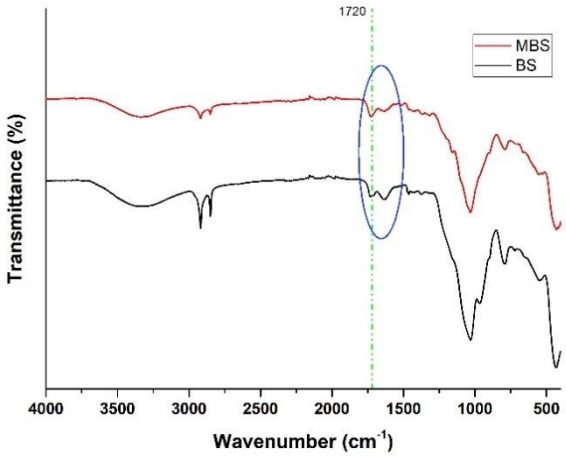

Figure 2 FTIR spectra of BS and MBS

Point of zero charges (pH_{PZC}) and pH studies

The pH at the point of zero charges (pH_{PZC}) is a preliminary assessment of the adsorbent surface charge, while the charge of the adsorbent surface is zero (Segovia-Sandoval et al., 2018). At

the lower value of $pH_{PZC,}$ the charge of the adsorbent surface is negative and positive above pH_{PZC} (Zaidi et al., 2018). Figure 3A shows the plot of the initial pH vs. final pH, wherein the pHpzc value of SB was obtained at around 3.19. The electrostatic interaction between the negatively charged adsorbent surface with Fe(III) ions is favored in the adsorption process. The pH dependence of equilibrium adsorption Fe(III) ions is investigated in the range 2 – 6, shown in Figure 3B. The results showed that the adsorption capacity of Fe(III) ions onto SB increases with rising pH and slightly decreases at higher pH. The optimum pH of the adsorption process using SB at pH 5. The negative charge of the adsorbent surface and deprotonation on the adsorbent increases cause increasing adsorption capacity, but with an increase in pH, the formation of soluble hydroxyl complexes could decrease the adsorption capacity (Pehlivan et al., 2012).

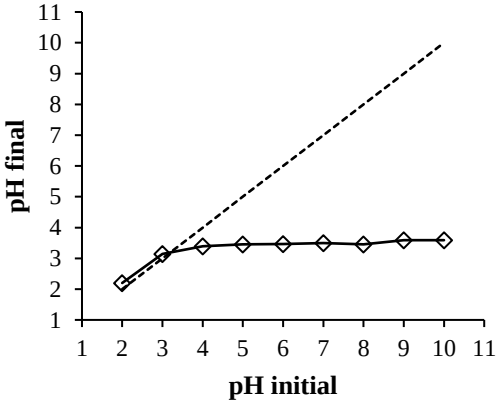

A

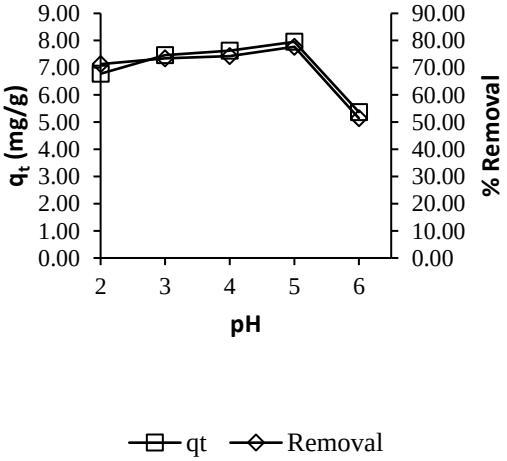

B

Figure 3 pH_{PZC} of MBS (A) and effect of pH on SB adsorption (B)

The impact of MBS dosage

To investigate the effect of MBS dosage, 0.6 – 6 $g.L^{-1}$ of MBS was used while keeping the other parameters constant, i.e., initial Fe(III) concentration of 300 $mg.L^{-1}$, pH 3, and continuous time of 60 min. Figure 4 shows that the percentage removal of Fe(III) increased with the increase in the adsorbent dose. On the other hand, the q_e decrease when the adsorbent dosage increase. These results may be due to the number of the active site on the MBS, whereas the decline indicated the aggregation and overlapping of adsorption sites (Kırbıyık et al., 2017).

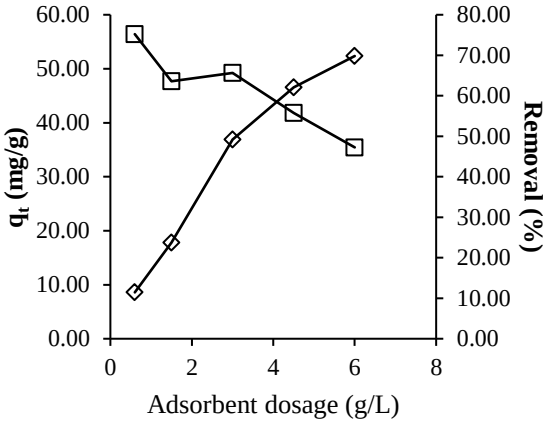

Figure 4 Effect of adsorbent dosage on Fe(III) removal using MBS

The effect of contact time

The effect of contact time was evaluated at intervals from 1 to 240 min while keeping other parameters (initial Fe(III) concentration 300 mg/L, pH 3, and adsorbent dosage 1.5 $mg.L^{-1}$). Figure 5 shows the effect of contact time on Fe(III) ion uptake by adsorbents. The Fe(III) uptake rate reaches equilibrium at 60 min contact time. The prolonged contact time may indicate that the adsorbent has a bigger capacity (Mariana et al., 2021). In the beginning, the adsorbent fast adsorb the Fe(III) until it reaches an equilibrium state. It is because of the large active sites on the MBS that easily interact with Fe(III) ions but with increasing time, the active sites become saturated (Sheibani et al., 2012).

Adsorption kinetics of Fe(III) on MBS

A kinetic study is needed regarding the mechanism of the adsorption process controlled by mass transfer (physical adsorption) or chemical adsorption. Adsorption kinetics modeling of Fe(III) adsorption onto MBS was carried out by

using the pseudo-first-order model (PFO), pseudo-second-order model (PSO), Elovich kinetics model, and intraparticle diffusion. The equation from each kinetics model can be seen in Table 1, while the value of the kinetics of Fe(III) ions adsorption on MBS is shown in Table 2. The summarized data from table 3, show that Fe(III) adsorption onto MBS fitted with PSO models (R^2 = 0.998) compare with other models (R^2 PFO = 0.393, Elovich = 0.793 and intraparticle diffusion = 0.572). These results indicate that Fe(III) removal may be controlled by a chemisorption process involving electrostatic forces (Sajjadi et al., 2019). The value of adsorption capacity of Fe(III) obtained from the experiment (q_{exp} = 14.759 $mg.g^{-1}$) quite similar with the value obtained from theoretical calculations ($q_{e,cal}$ = 14.970 $mg.g^{-1}$) using the PSO model. These results are also supported by the Elovich model, where the chemisorption rate is 17.252 $mg.g^{-1}.min^{-1}$ and surface coverage 0.452 $g.mg^{-1}$.

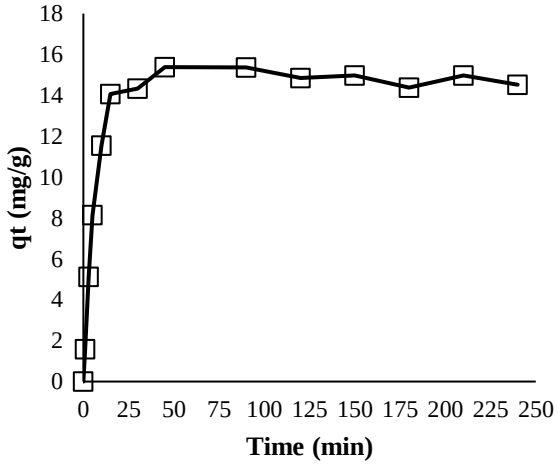

Figure 5 The plot of the amount of Fe(III) ion uptake with MBS

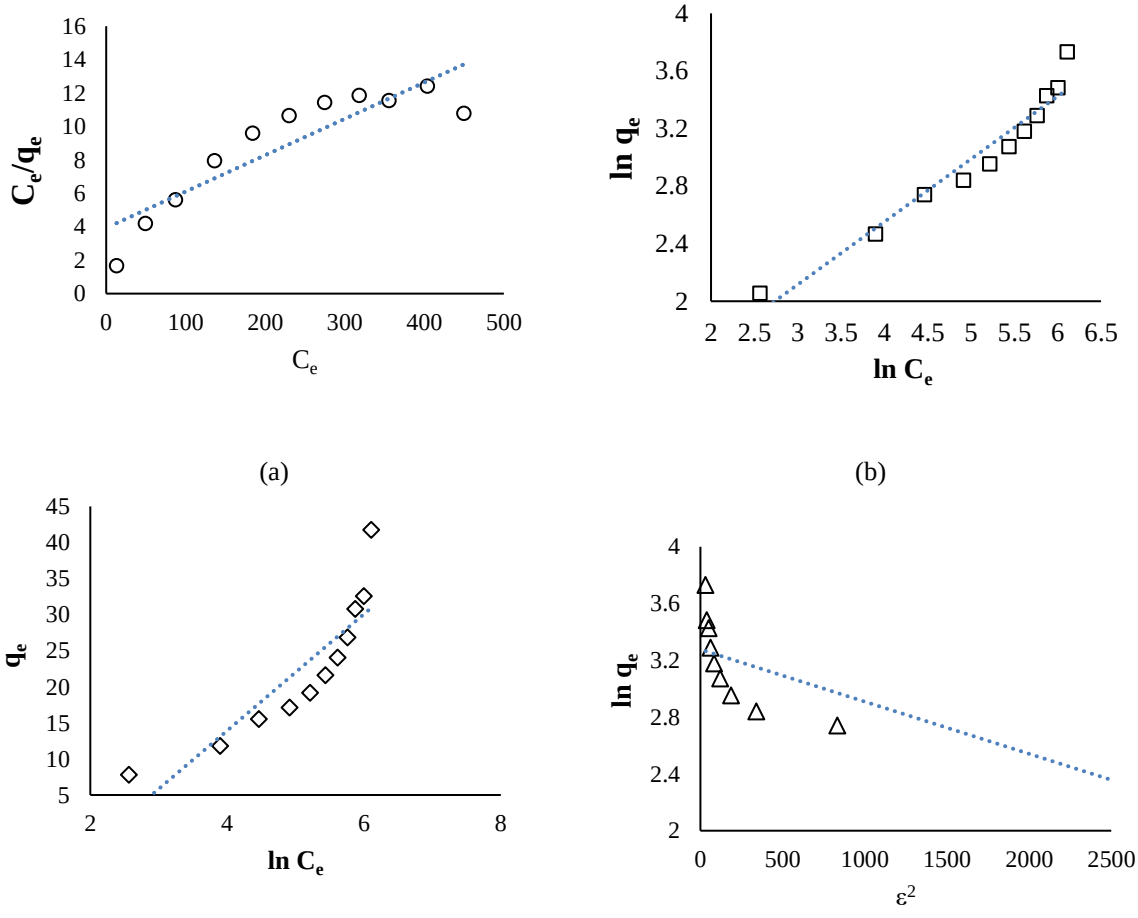

(a) (b)

(c) (d)

Figure 6 Langmuir (a), Freundlich (b), Temkin (c), and Dubinin–Radushkevich (D–R) (d) isotherm for the removal of Fe (III) onto MBS

Table 3 The value of the kinetics of Fe(III) ions adsorption on MBS

Kinetic models	Parameters	Value
PFO	R^2	0.393
	K_1 (min^{-1})	0.0027
	q_e ($mg.g^{-1}$)	14.365
PSO	R^2	0.998
	K_2 (min^{-1})	0.025
	q_e ($mg.g^{-1}$)	14.970
Elovich	R^2	0.793
	α ($mg.g^{-1}$. min^{-1})	17.252
	β ($g.mg^{-1}$)	0.452
Intraparticle diffusion	R^2	0.572
	K_{id} ($mg.g^{-1}$. $min^{-0.5}$)	0.755
	C ($mg.g^{-1}$)	5.966

Table 4 Comparison of Fe(III) adsorption using MBS adsorbent with various other adsorbents that have been previously reported.

Adsorbent	pH	qe ($mg. g^{-1}$)	Ref
Carbon from Tamarind seed	7.9	0.0069	(Mopoung et al., 2015)
Sago-Kaoline Dregs	4	1.689	(Cici et al., 2017)
Chitosan films	4.5	621.2	(Marques et al., 2018)
Cocoa (Theobroma cacao) Pod Husk	7.5	4.16	(Obike et al., 2018)
Orange peel	9	0.037	(Rifat Mamun et al., 2019)
Tea leaves		42.37	
Modified Candlenut Shell	5	15.15	(Simanjuntak et al., 2020)
Modifies bagasse sorghum (This study)	5	45.872	

Adsorption Isotherm of Fe(III) on MBS

The interaction between the adsorbate and adsorbent that give results favorable or unfavorable can be determined by the isotherm shape. The experimental sorption equilibrium data uses four isotherm models, including Langmuir, Freundlich, Temkin, and Dubinin–Radushkevich (D–R). The isotherm models and the results of the isothermal modeling are shown in Table 2. The plotted graphs of Langmuir, Freundlich, Temkin, and Dubinin–Radushkevich (D–R) isotherm for removing Fe (III) onto MBS are shown in Figure 6. Based on the results, it can be seen from the correlation that the isotherm adsorption of Fe(III) on MBS occurs with the Freundlich isotherm model (R^2 = 0.941). The Freundlich models parameter shows n and $K_{F,}$ representing the adsorption intensity and the adsorption capacity, respectively(Foroutan et al., 2018). These suggested that the mechanism of the adsorption process on the adsorbent was heterogeneous and multilayer. From Table 3, the maximum adsorption capacity based on Langmuir models was estimated at around 45.872 $mg.g^{-1}$. The comparison of the performance of the adsorbent with other adsorbents in the adsorption of Fe(III) is presented in table 4. Table 4 shows that waste biomass performed adsorption on Fe(III) with different pH and various level adsorption capacities; the qe value of MBS can compete with other adsorbents. Modified Candlenut Shell has the same pH parameter as MBS but with lower absorption capacity; this indicates that MBS can be used as a potential candidate adsorbent to adsorb Fe (III).

CONCLUSION

This study investigated the adsorption performance of MBS to remove Fe(III) ions. The MBS was characterized by FESEM, FTIR, and BET surface area analyses. The morphology of MBS shows that the porosity and voids were

increased after treatment using citric acid. The FTIR results for MBS described that carboxyl and hydroxyl contribute to the Fe(III) adsorption on MBS. The BET results in a surface area of 0.290 m2/g with total pores of 0.0015 cm^3/g. In batch equilibrium studies, the maximum adsorption capacity was obtained at 5 pH values, 45.875 mg. $g^{-1,}$ and 60 min contact time at room temperature. The kinetics models of Fe(III) onto MBS follow pseudo-second-order (PSO) and are supported by the Elovich model. The Freundlich model fitted better than the other models. Overall, the MBS has shown its potential as an effective and low-cost adsorbent for removing Fe(III) from an aqueous solution.

ACKNOWLEDGEMENT

The authors would like to thank the Integrated Laboratory of Bioproduct (iLab) National Research and Innovation Agency (NRIA).

REFERENCES

Almasi, A., M. Omidi, M. Khodadadian, R. Khamutian, and M.B. Gholivand. 2012. Lead(II) and cadmium(II) removal from aqueous solution using processed walnut shell: kinetic and equilibrium study. http://dx.doi.org/10.1080/02772248.2012.671328. 94(4):660–671.

Anbia, M., and S. Amirmahmoodi. 2016. Removal of Hg (II) and Mn (II) from aqueous solution using nanoporous carbon impregnated with surfactants. Arabian Journal of Chemistry. 9:S319–S325.

Azizian, S., and R.N. Fallah. 2010. A new empirical rate equation for adsorption kinetics at solid/solution interface. Applied Surface Science. 256(17):5153–5156.

Candido, R.G., and A.R. Gonçalves. 2016. Synthesis of cellulose acetate and carboxymethylcellulose from sugarcane straw. Carbohydrate Polymers. 152:679–686.

Cici, I., L. Destiarti, and A. Shofiyani. 2017. Pemanfaatan komposit ampas sagu-kaolin untuk adsorpsi Fe(II). Jurnal Kimia dan Kemasan. 6(2):7–13.

Das, N., R. Vimala, and P. Karthika. 2008. Biosorption of heavy metals–An overview. IJBT Vol.7(2) [April 2008]. 7:159–169.

Dungani, R., M. Karina, Subyakto, A. Sulaeman, D. Hermawan, and A. Hadiyane. 2016. Agricultural waste fibers towards sustainability and advanced utilization: a review. Asian Journal of Plant Sciences. 15(1/2):42–55.

Foroutan, R., H. Esmaeili, A.M. Sanati, M. Ahmadi, and B. Ramavandi. 2018. Adsorptive removal of Pb(II), Ni(II), and Cd(II) from aqueous media and leather wastewater using Padinasanctae-crucis biomass. Desalination and Water Treatment. 135:236–246.

Ghosh, P., A.N. Samanta, and S. Ray. 2011. Reduction of COD and removal of Zn2+ from rayon industry wastewater by combined electro-Fenton treatment and chemical precipitation. Desalination. 266(1–3):213–217.

De Gisi, S., G. Lofrano, M. Grassi, and M. Notarnicola. 2016. Characteristics and adsorption capacities of low-cost sorbents for wastewater treatment: A review. Sustainable Materials and Technologies. 9:10–40.

Hoang, M.T., TD. Pham, T.T. Pham, M.K. Nguyen, D.T.T. Nu, T.H. Nguyen, S. Bartling, and B. Van der Bruggen. 2021. Esterification of sugarcane bagasse by citric acid for Pb2+ adsorption: effect of different chemical pre-treatment methods. Environmental Science and Pollution Research. 28(10):11869–11881.

Jóźwiak, T., U. Filipkowska, J. Struk-Sokołowska, K. Bryszewski, K. Trzciński, J. Kuźma, and M. Ślimkowska. 2021. The use of spent coffee grounds and spent green tea leaves for the removal of cationic dyes from aqueous solutions. Scientific Reports 2021 11:1. 11(1):1–12.

Khosravihaftkhany, S., N. Morad, A.Z. Abdullah, T.T. Teng, and N. Ismail. 2015. Biosorption of Pb(II) and Fe(III) from aqueous co-solutions using chemically pretreated oil palm fronds. RSC Advances. 5(129):106498–106508.

Kırbıyık, Ç., A.E. Pütün, and E. Pütün. 2017. Equilibrium, kinetic, and thermodynamic studies of the adsorption of Fe(III) metal ions and 2,4-dichlorophenoxyacetic acid onto biomass-based activated carbon by ZnCl2 activation. Surfaces and Interfaces. 8:182–192.

Leon, V.B. de, B.A.F. de Negreiros, C.Z. Brusamarello, G. Petroli, M. Di Domenico,

and F.B. de Souza. 2020. Artificial neural network for prediction of color adsorption from an industrial textile effluent using modified sugarcane bagasse: Characterization, kinetics and isotherm studies. Environmental Nanotechnology, Monitoring & Management. 14:100387.

Liu, Y., J. Wei, Y. Tian, and S. Yan. 2015. The structure–property relationship of manganese oxides: highly efficient removal of methyl orange from aqueous solution. Journal of Materials Chemistry A. 3(37):19000–19010.

Lo, S.F., S.Y. Wang, M.J. Tsai, and L.D. Lin. 2012. Adsorption capacity and removal efficiency of heavy metal ions by Moso and Ma bamboo activated carbons. Chemical Engineering Research and Design. 90(9):1397–1406.

Mariana, M., F. Mulana, L. Juniar, D. Fathira, R. Safitri, S. Muchtar, M.R. Bilad, A.H.M. Shariff, and N. Huda. 2021. Development of biosorbent derived from the endocarp waste of gayo coffee for lead removal in liquid wastewater-effects of chemical activators. Sustainability (Switzerland). 13(6).

Mariana, M., F. Mulana, S. Sofyana, N.P. Dian, and M.R. Lubis. 2019. Characterization of adsorbent derived from Coconut Husk and Silica (SiO2). IOP Conference Series: Materials Science and Engineering. 523(1):012022.

Marques, J.L., S.F. Lütke, T.S. Frantz, J.B.S. Espinelli, R. Carapelli, L.A.A. Pinto, and T.R.S. Cadaval. 2018. Removal of Al (III) and Fe (III) from binary system and industrial effluent using chitosan films. International Journal of Biological Macromolecules. 120:1667–1673.

Monroy-Figueroa, J., D.I. Mendoza-Castillo, A. Bonilla-Petriciolet, and M.A. Pérez-Cruz. 2014. Chemical modification of Byrsonima crassifolia with citric acid for the competitive sorption of heavy metals from water. International Journal of Environmental Science and Technology 2014 12:9. 12(9):2867–2880.

Mopoung, S., P. Moonsri, W. Palas, and S. Khumpai. 2015. Characterization and Properties of Activated Carbon Prepared from Tamarind Seeds by KOH Activation for Fe(III) Adsorption from Aqueous Solution. Scientific World Journal. 2015.

Neolaka, Y.A.B., Y. Lawa, J. Naat, A.A.P. Riwu, Y.E. Lindu, H. Darmokoesoemo, B.A. Widyaningrum, M. Iqbal, and H.S. Kusuma. 2021. Evaluation of magnetic material IIP@GO-Fe3O4 based on Kesambi wood (Schleichera oleosa) as a potential adsorbent for the removal of Cr(VI) from aqueous solutions. Reactive and Functional Polymers. 166(July):105000.

Nurfahmi, H.C. Ong, B.M. Jan, C.W. Tong, H. Fauzi, and W.H. Chen. 2016. Effects of organosolv pre-treatment and acid hydrolysis on palm empty fruit bunch (PEFB) as bioethanol feedstock. Biomass and Bioenergy. 95:78–83.

Nurhayatun Nafsiyah, Anis Shofiyani, I.S. 2017. Studi Kinetika dan Isoterm Adsorpsi Fe(III) pada Bentonit Teraktivasi Asam Sulfat. Jurnal Kimia dan Kemasan. 6(1):57–63.

Obike, A.I., J.C. Igwe, C.N. Emeruwa, and K.J. Uwakwe. 2018. Equilibrium and kinetic studies of Cu (II), Cd (II), Pb (II) and Fe (II) adsorption from aqueous solution using cocoa (*Theobroma cacao*) pod husk. Journal of Applied Sciences and Environmental Management. 22(2):182.

Oliveira, M.R.F., K. do Vale Abreu, A.L.E. Romão, D.M.B. Davi, C.E. de Carvalho Magalhães, E.N.V.M. Carrilho, and C.R. Alves. 2021. Carnauba (Copernicia prunifera) palm tree biomass as adsorbent for Pb(II) and Cd(II) from water medium. Environmental Science and Pollution Research. 28(15):18941–18952.

Pehlivan, E., T. Altun, and S. Parlayici. 2012. Modified barley straw as a potential biosorbent for removal of copper ions from aqueous solution. Food Chemistry. 135(4):2229–2234.

Qu, J., Y. Liu, L. Cheng, Z. Jiang, G. Zhang, F. Deng, L. Wang, W. Han, and Y. Zhang. 2021. Green synthesis of hydrophilic activated carbon supported sulfide nZVI for enhanced Pb(II) scavenging from water: Characterization, kinetics, isotherms and mechanisms. Journal of Hazardous Materials. 403:123607.

Rifat Mamun, K., N. Kumar Saha, and S. Chakrabarty. 2019. A Comparative Study of the Adsorption Capacity of Tea Leaves

and Orange Peel for the Removal of Fe (III) Ion from Wastewater. Journal of Chemical Health Risks. 9(2):107–115.

Sajjadi, S.A., A. Meknati, E.C. Lima, G.L. Dotto, D.I. Mendoza-Castillo, I. Anastopoulos, F. Alakhras, E.I. Unuabonah, P. Singh, and A. Hosseini-Bandegharaei. 2019. A novel route for preparation of chemically activated carbon from pistachio wood for highly efficient Pb(II) sorption. Journal of Environmental Management. 236:34–44.

Segovia-Sandoval, S.J., R. Ocampo-Pérez, M.S. Berber-Mendoza, R. Leyva-Ramos, A. Jacobo-Azuara, and N.A. Medellín-Castillo. 2018. Walnut shell treated with citric acid and its application as biosorbent in the removal of Zn(II). Journal of Water Process Engineering. 25(March):45–53.

Shaidan, N.H., U. Eldemerdash, and S. Awad. 2012. Removal of Ni(II) ions from aqueous solutions using fixed-bed ion exchange column technique. Journal of the Taiwan Institute of Chemical Engineers. 43(1):40–45.

Sheibani, A., M.R. Shishehbor, and H. Alaei. 2012. Removal of Fe(III) ions from aqueous solution by hazelnut hull as an adsorbent. International Journal of Industrial Chemistry. 3(1):1–3.

Simanjuntak, R., P. Taba, R. Ibrahim, E. Bahsar Demmallino, and C. Author. 2020. Effectiveness of Modified Candlenut Shell (Alleurites mollucana) in Adsorption of Fe (III) Heavy Metals to Improve Groundwater Quality. Advances in Environmental Biology. 14(1):36–41.

Suhendrayatna, S., and M. Zaki. (n.d.). Adsorption of Manganese (II) Ion in the Water Phase by Citric Acid Activated Carbon of Rice Husk Preparation of Activated Carbon from rice husk as an adsorbent View project.

Sun, RC 2010. Cereal Straw as a Resource for Sustainable Biomaterials and Biofuels. Page Cereal Straw as a Resource for Sustainable Biomaterials and Biofuels.

Tahoon, M.A., S.M. Siddeeg, N.S. Alsaiari, W. Mnif, and F. Ben Rebah. 2020, May 29. Effective heavy metals removal fromwater using nanomaterials: A review. Multidisciplinary Digital Publishing Institute.

Tan, I.A.W., J.C. Chan, B.H. Hameed, and L.L.P. Lim. 2016. Adsorption behavior of cadmium ions onto phosphoric acid-impregnated microwave-induced mesoporous activated carbon. Journal of Water Process Engineering. 14:60–70.

Tejada-Tovar, C., A. Villabona-Ortíz, R. Ortega-Toro, H. Mancilla-Bonilla, and F. Espinoza-León. 2021. Potential Use of Residual Sawdust of Eucalyptus globulus Labill in Pb (II) Adsorption: Modelling of the Kinetics and Equilibrium. Applied Sciences 2021, Vol. 11, Page 3125. 11(7):3125.

Wan Ngah, W.S., and M.A.K.M. Hanafiah. 2008. Removal of heavy metal ions from wastewater by chemically modified plant wastes as adsorbents: A review. Bioresource Technology. 99(10):3935–3948.

Wang, F.H., H.T. Hao, R. fei Sun, S. yin Li, R. ming Han, C. Papelis, and Y. Zhang. 2014. Bench-scale and pilot-scale evaluation of coagulation pre-treatment for wastewater reused by reverse osmosis in a petrochemical circulating cooling water system. Desalination. 335(1):64–69.

Wartelle, L.H., and W.E. Marshall. 2000. Citric acid modified agricultural by-products as copper ion adsorbents. Advances in Environmental Research. 4(1):1–7.

Xu, X., X. Cao, and L. Zhao. 2013. Comparison of rice husk- and dairy manure-derived biochars for simultaneously removing heavy metals from aqueous solutions: Role of mineral components in biochars. Chemosphere. 92(8):955–961.

Zaidi, N.A.H.M., L.B.L. Lim, and A. Usman. 2018. Enhancing adsorption of Pb(II) from aqueous solution by NaOH and EDTA modified Artocarpus odoratissimus leaves. Journal of Environmental Chemical Engineering. 6(6):7172–7184.